Finite Element Methods for Modern Engineering Applications

Shuvodeep De
Engineering Technology
Texas State University

Background and Research Interest

- **Keywords**: Solid Mechanics • Multiphysics Simulation • Surface/Interfaces
- Finite Element Analysis (FEA) • Biomimetics
- **Selected Research Projects**:
  - Bio-inspired Aircraft Wings
  - Advanced Truck-chassis Design
  - Electrodeposition with Additives for Fabrication of Interconnects
  - Tribology of additively manufactured outsoles tread designs
  - Gecko-inspired Surface Microstructures

Bio-inspired Design of Aircraft Wings [1-5]

Motivation

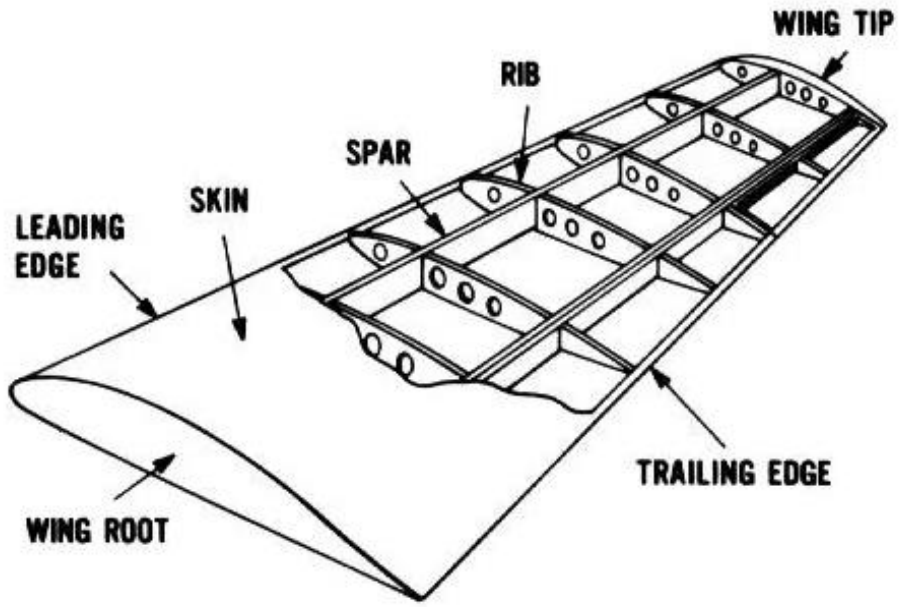

Wing Internal Structure[#]

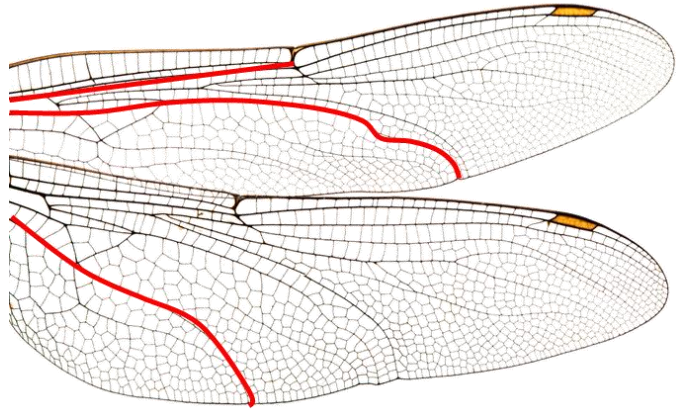

Dragonfly wing *

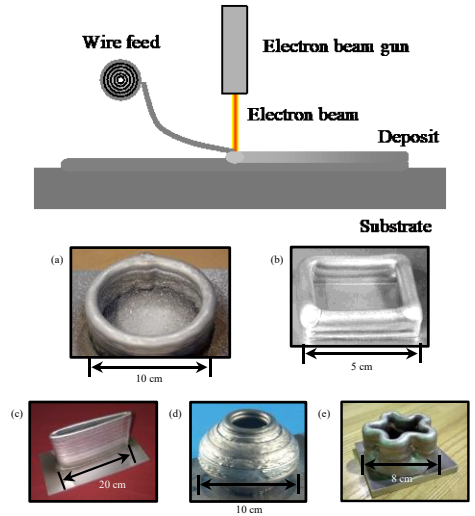

EBF3 in 0-g experiment (Courtesy: Taminger)

Electronic beam free form fabrication (EBF3) for 3D printing, (Taminger and Hafley 2003)

- Biologically inspired arbitrarily shaped stiffeners for structural design
- Stringers (veins) along wing are not always straight, which are mixed by curved and straight stringers
- Development of additive manufacturing technology for 3D printings of metal structures

[#] https://pdxscholar.library.pdx.edu/honorstheses/538/
*http://www.publicdomainpictures.net/viewimage.php?image=25114&picture=&jazyk=CN

Wing Optimization Problem

Objective: Reduce structural weight satisfying Constraints

Aeroelastic Load Approximated

- Vortex-Lattice method
- Cruise Speed: Mach 0.85 at 35000 ft
- Angle of Attack: -2, 0, 2, 4, 6 degrees
- Total Span 192.7 ft
- Aspect Ratio AR = 9.0
- Quarter-Chord Sweep 35 Degrees

Static Constraints

- Stress < Yield Strength
- Maximum Displacement < 12.5% Span
- Twist Angle at Wing Tip < 6 Degrees

Bucking Constraints

- Buckling Factor of each panel >1
- Buckling Factor of entire wing >1

Flutter Analysis

Flutter Constraint:: Dynamic Pressure >1.75×1.2 psi

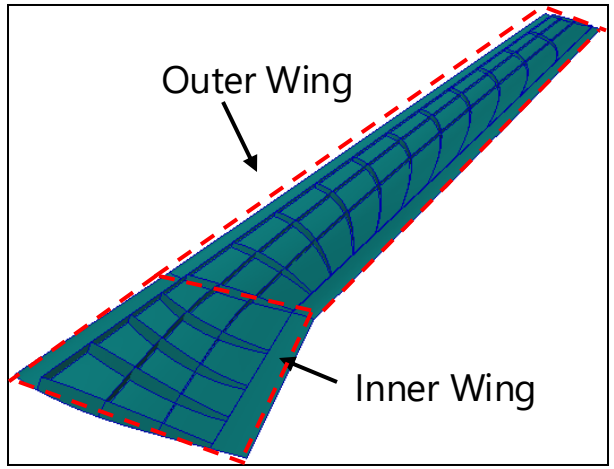

Parametric Wing Structure

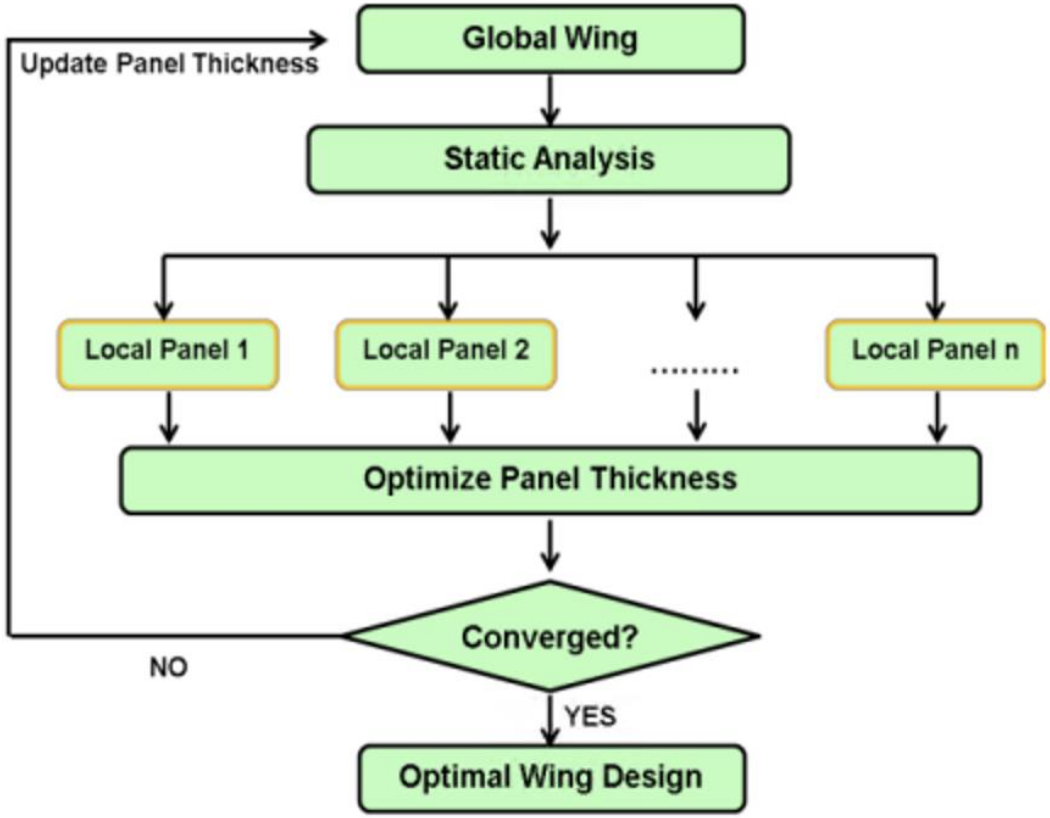

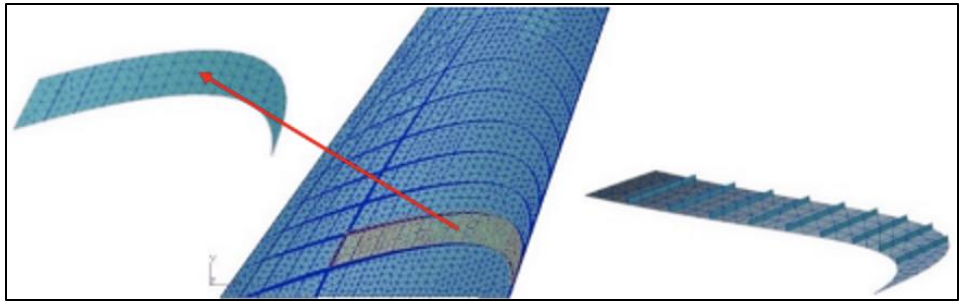

Domain Decomposition

Optimization Results

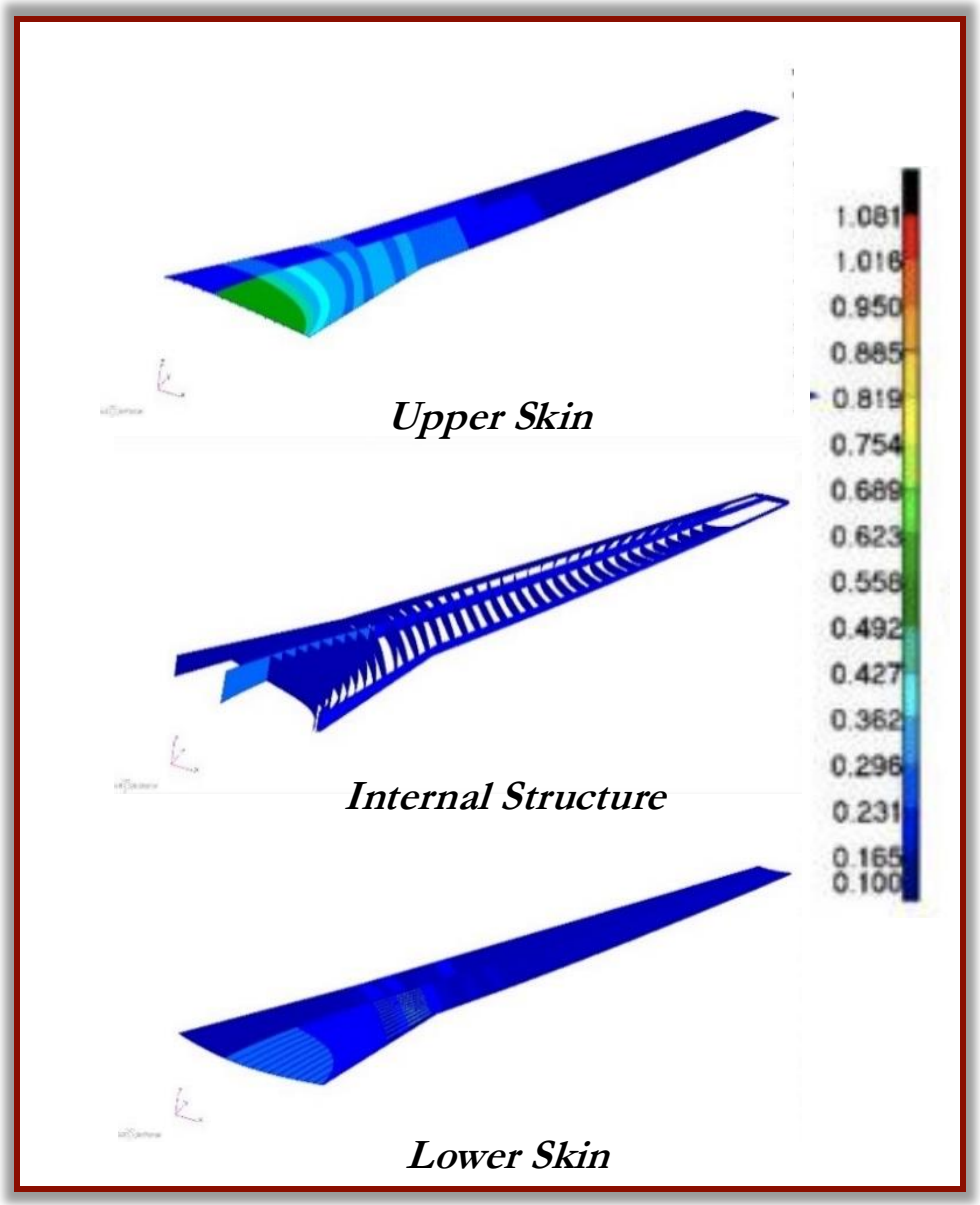

Structural Properties for Best Design

Properties	Value
Structural Weight	11002 lb
St. Weight reduction WRT Baseline	4%
Buckling Factor for AOA 6 degree	1.001 (satisfied)
Buckling Factor for AOA -2 degree	1.05 (satisfied)
Freq. for First Bending Mode	1.29 Hz
Freq. for First Torsional Mode	9.32 Hz
Maximum von Mises Stress	48100 psi (satisfied)
Flutter Velocity (knots)	612 knots (satisfied)

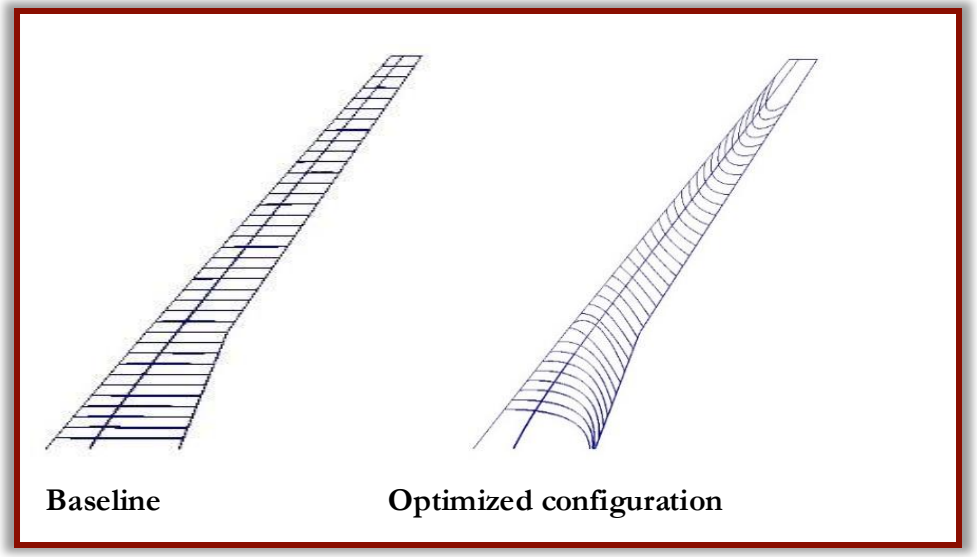

Lightweight Chassis design for Hybrid Super Trucks [6-8]

Motivation

Reduce the structural weight of commercial vehicle chassis:

- Highly complex mechanical assembly consisting of side-rail, mountings and several cross-member
- Static analysis for each design corresponding to various road conditions
- Parameterization of geometry using large number of design variables
- Incorporating several constraints – stress, modal frequency and stiffness
- Python script to automate geometry and mesh generation, analysis, evaluation of constraints

Typical Truck Chassis

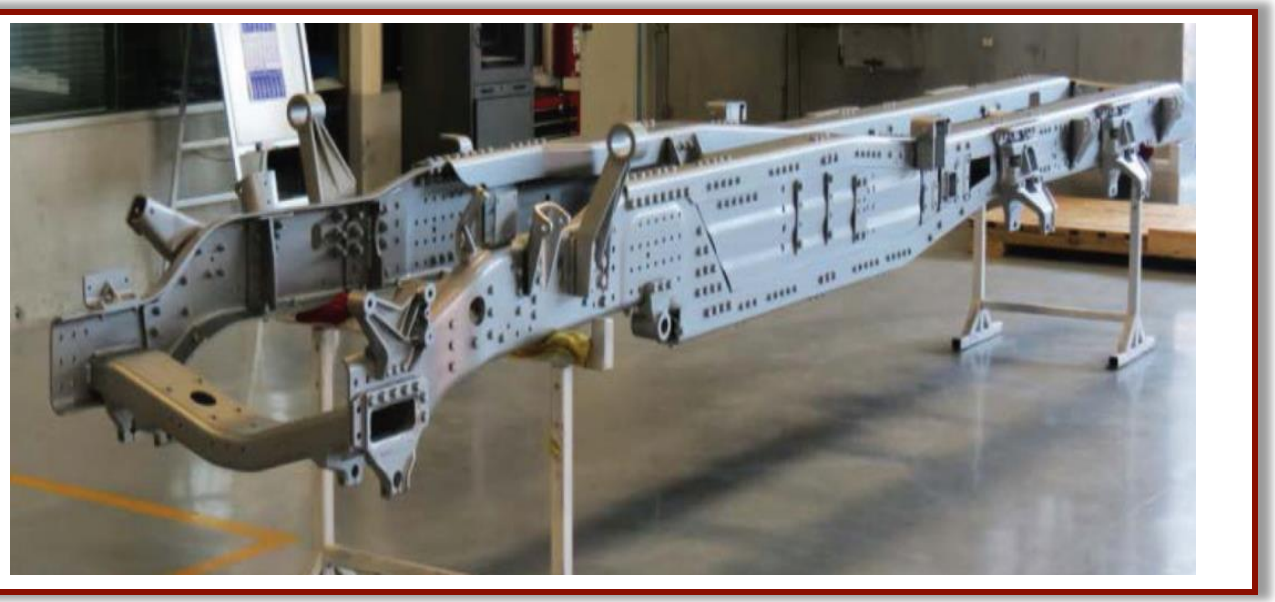

Light-weight Truck chassis prototype (Source: Metalsa)

Hybrid Truck Chassis Optimization Problem

Goals

- Develop physics based parametric model of truck chassis
- Minimize total Structural Weight of the frame by size and shape optimization
- Use multiple possible road conditions for static analysis (stress computation)

Design Parameters

- **Shape Variables**: Defines shape of the rail, internal brackets, hole diameters (range consistent with manufacturing capabilities)
- **Thickness Design Variables**: Thickness of different components (range consistent with available grade of sheet metals)

Constraints

- Violation of von Mises Stress criteria over less than 0.01 % surface area
- Geometric Constraints (e.g., Suspension should attach to the main rail)
- Vertical bending natural frequency > 20 Hz

Note: Due to stress singularities at certain points the maximum von Mises stress is often too high and thus design is based on stress violation factor

Optimization Framework

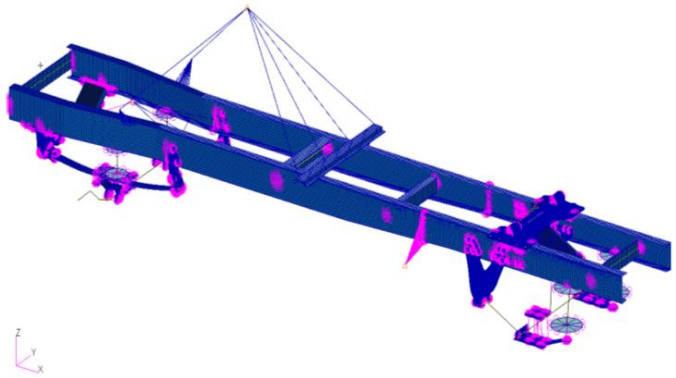

FEA Model of a Commercial Vehicle Chassis

$$Obj = w + 10^6\left(\sum max(0, g_i)^2\right)$$

Objective function:

$$g_1 = \frac{Violation}{0.001} - 1$$

$$g_2 = \frac{f_v}{20} - 1$$

Where:

- Violation is percentage surface area where von Mises stress constraint violated
- W is total weight of frame
- f_v is vertical bending natural frequency

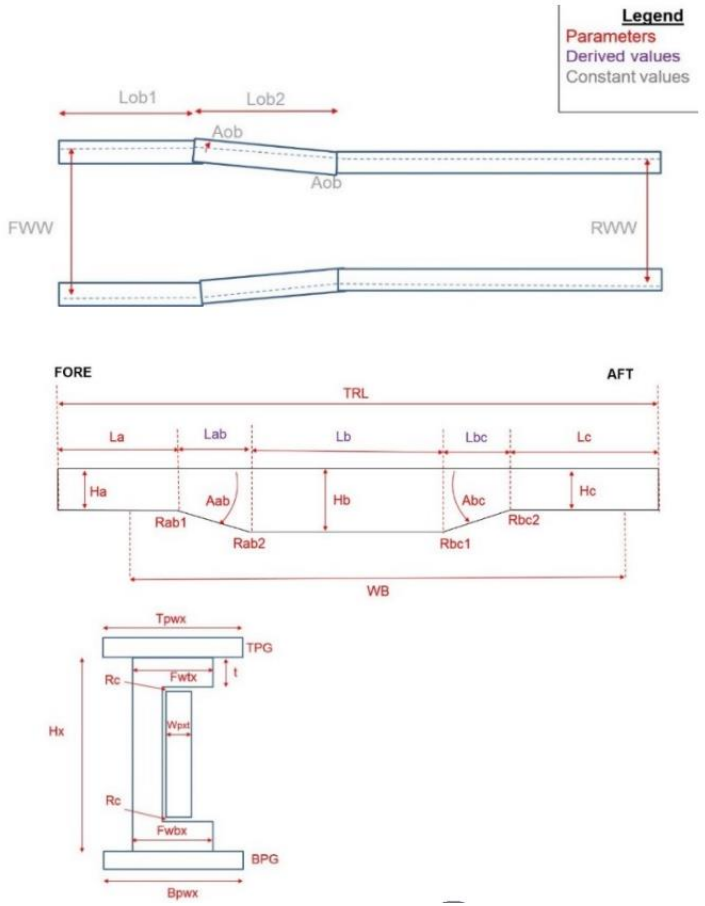

Geometry Parametrization

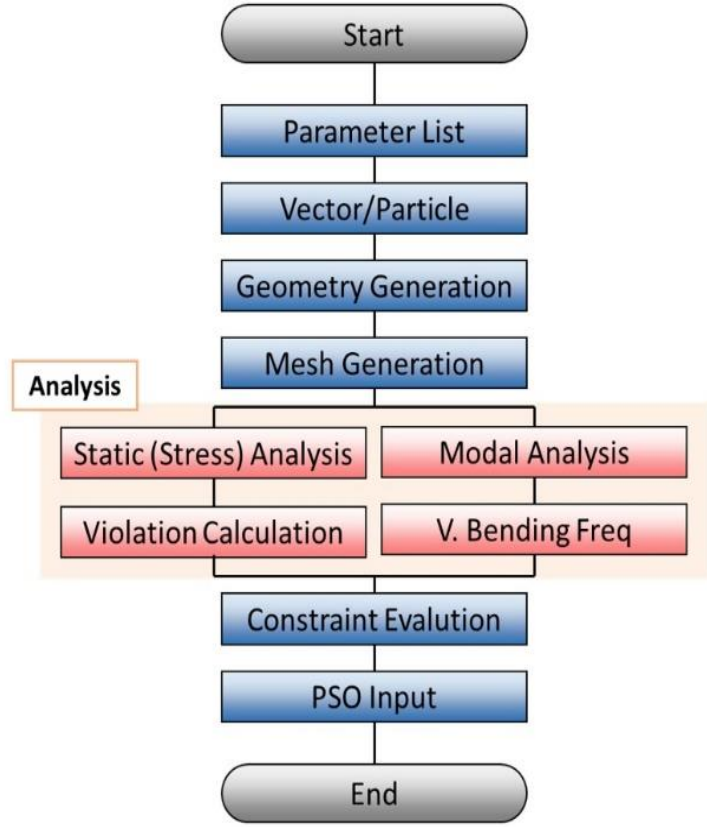

Code Structure

Optimization Results

- Optimized design has mass 275 Kg (13.25% less than baseline design)
- Vertical bending frequency and max Violation 20.5 Hz and 0.0086, respectively (close to constraint values)

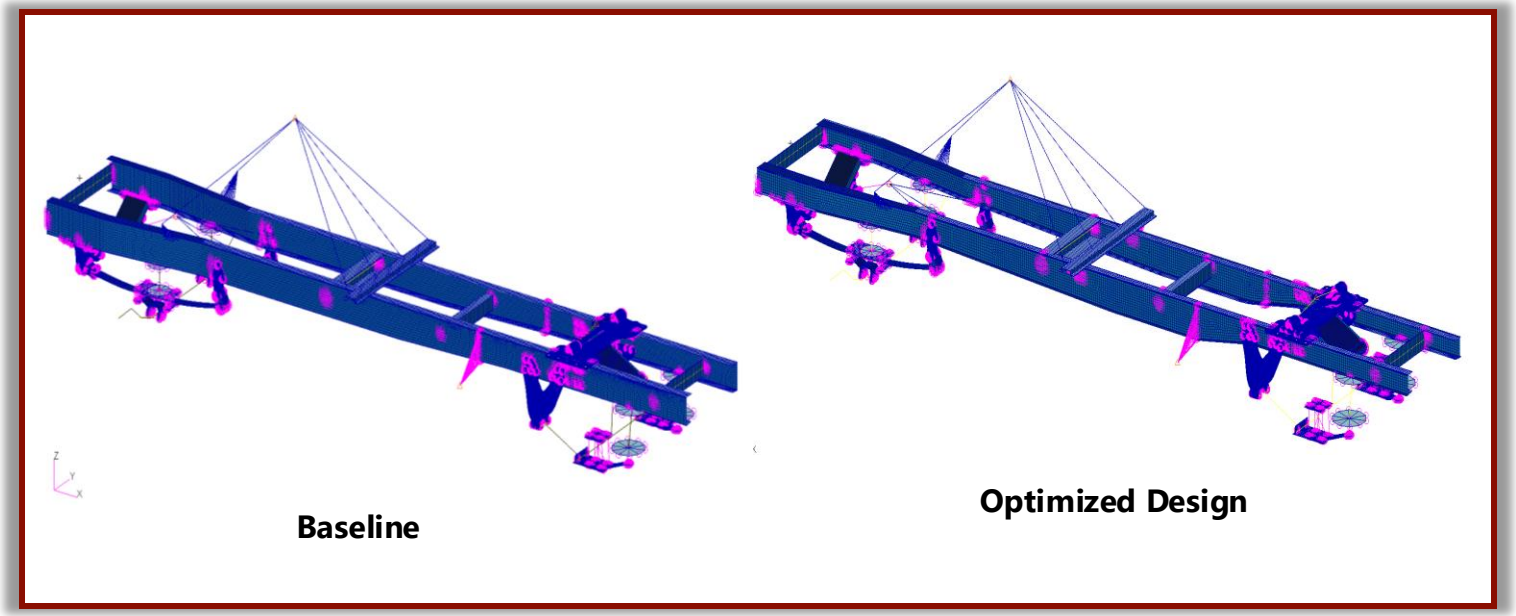

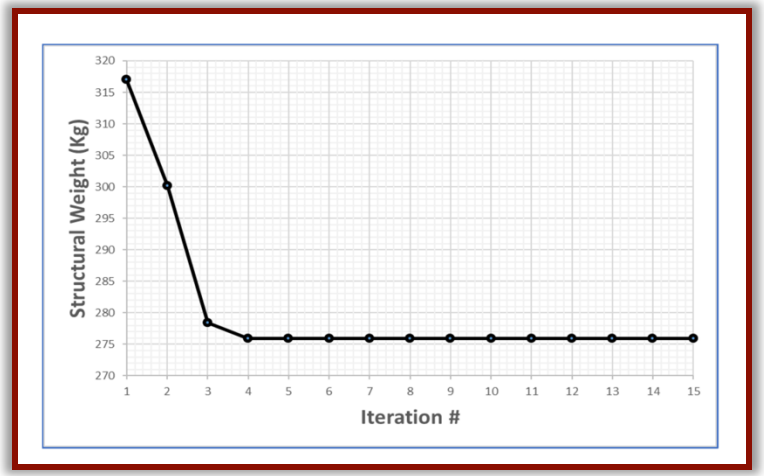

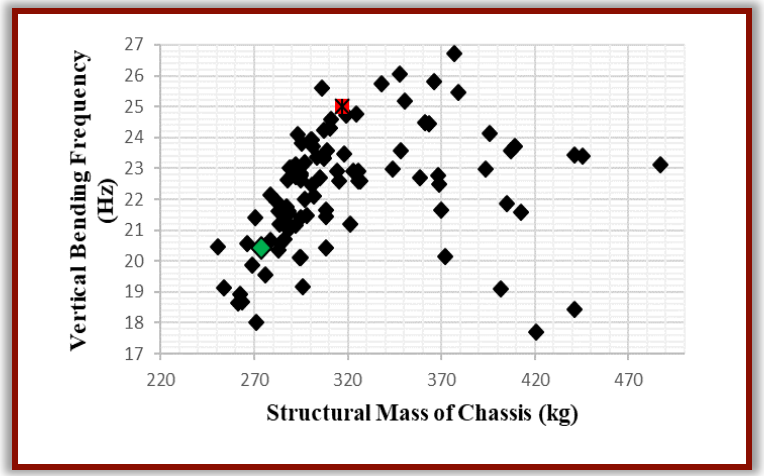

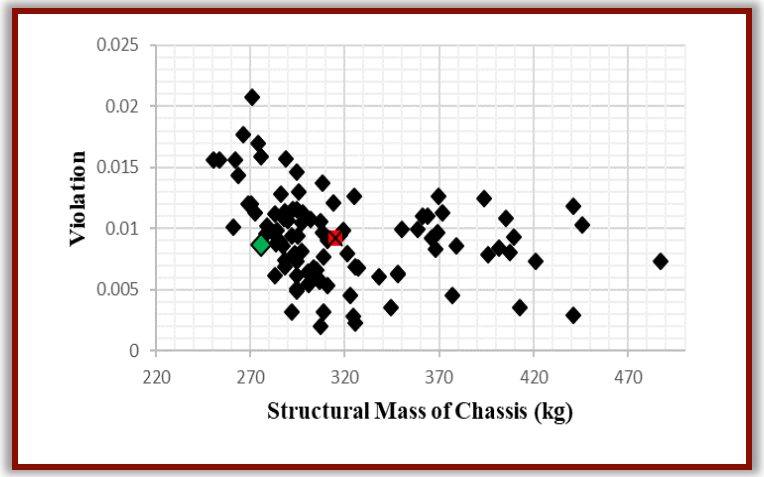

VIRGINIA TECH

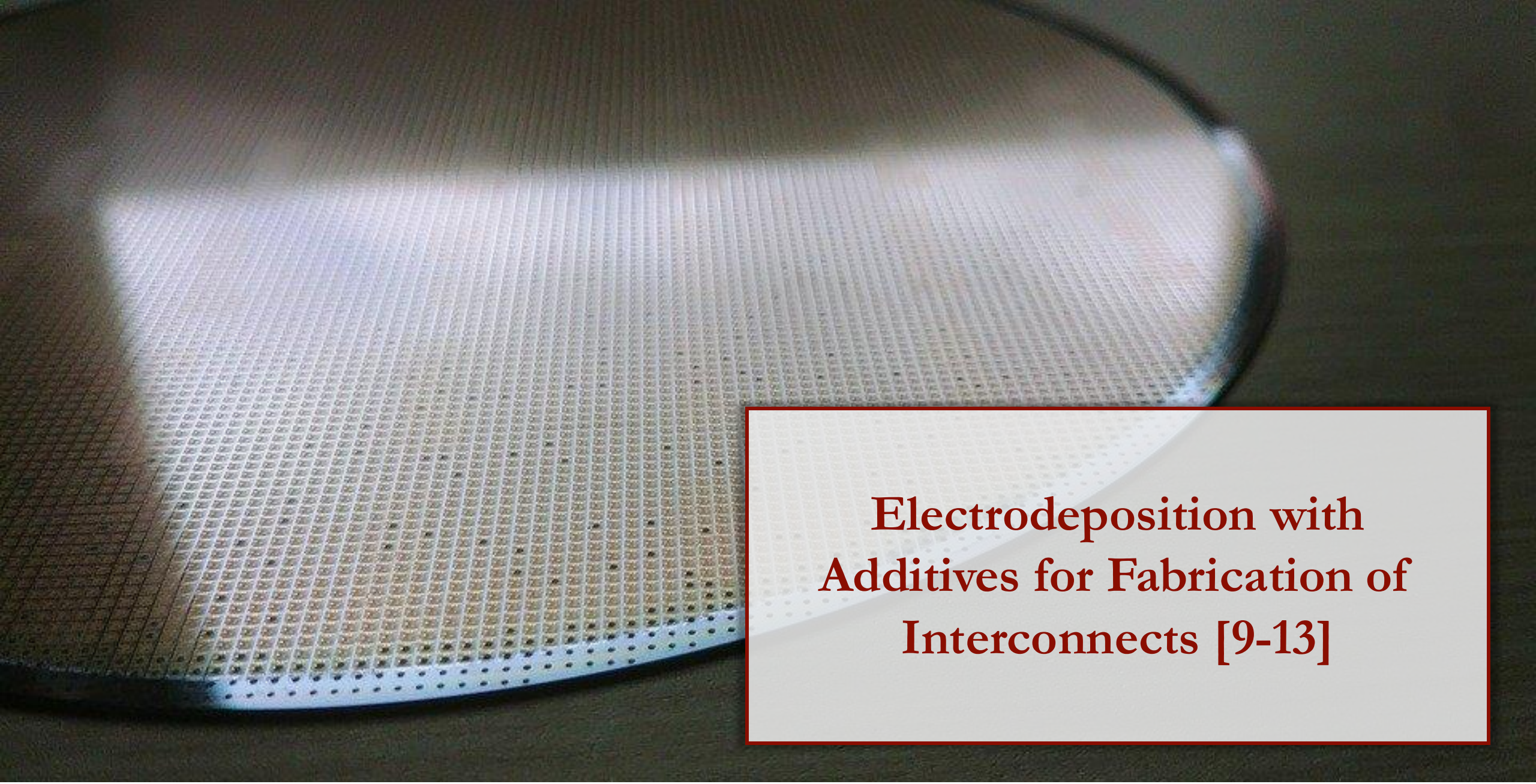

Electrodeposition with Additives for Fabrication of Interconnects [9-13]

Motivation

- Manufacturing of interconnects done by electrodeposition of metals in micro-trenches with fluid flow
- Organic additives (which modifies the current) applied to obtain defect-free "flat" deposition
- Challenging to find appropriate organic additives
- Simulation of the process using can expedite the research and development
- Process simulation / prediction requires determination of kinetic parameters (of Cu and additives)

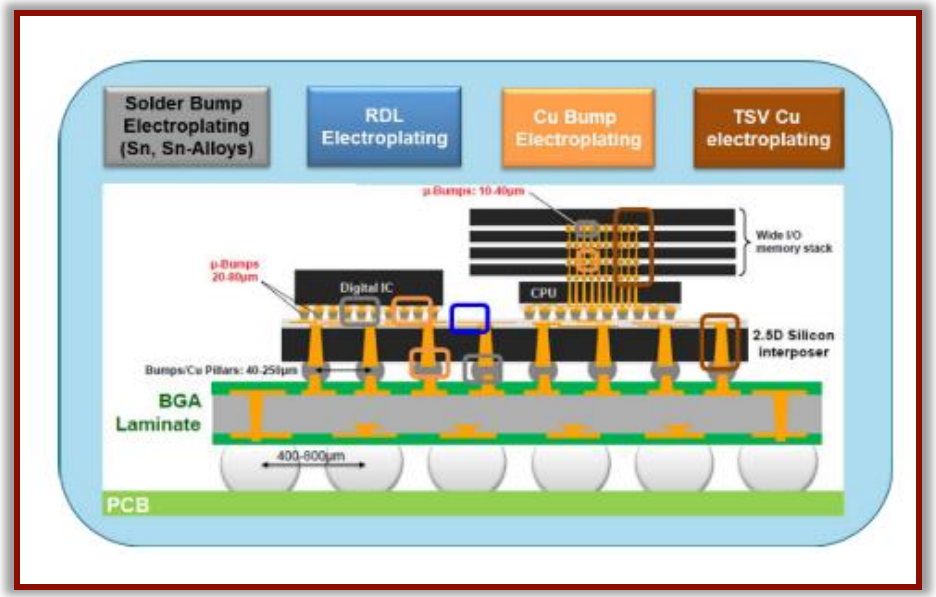

Copper Packaging (Source: BASF)

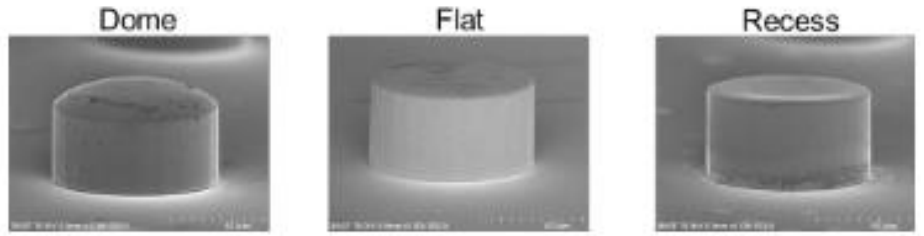

Different Copper Micro Bumps due to fluid flow and additives (Source: BASF)

Physiochemical Model (with Organic Additive)

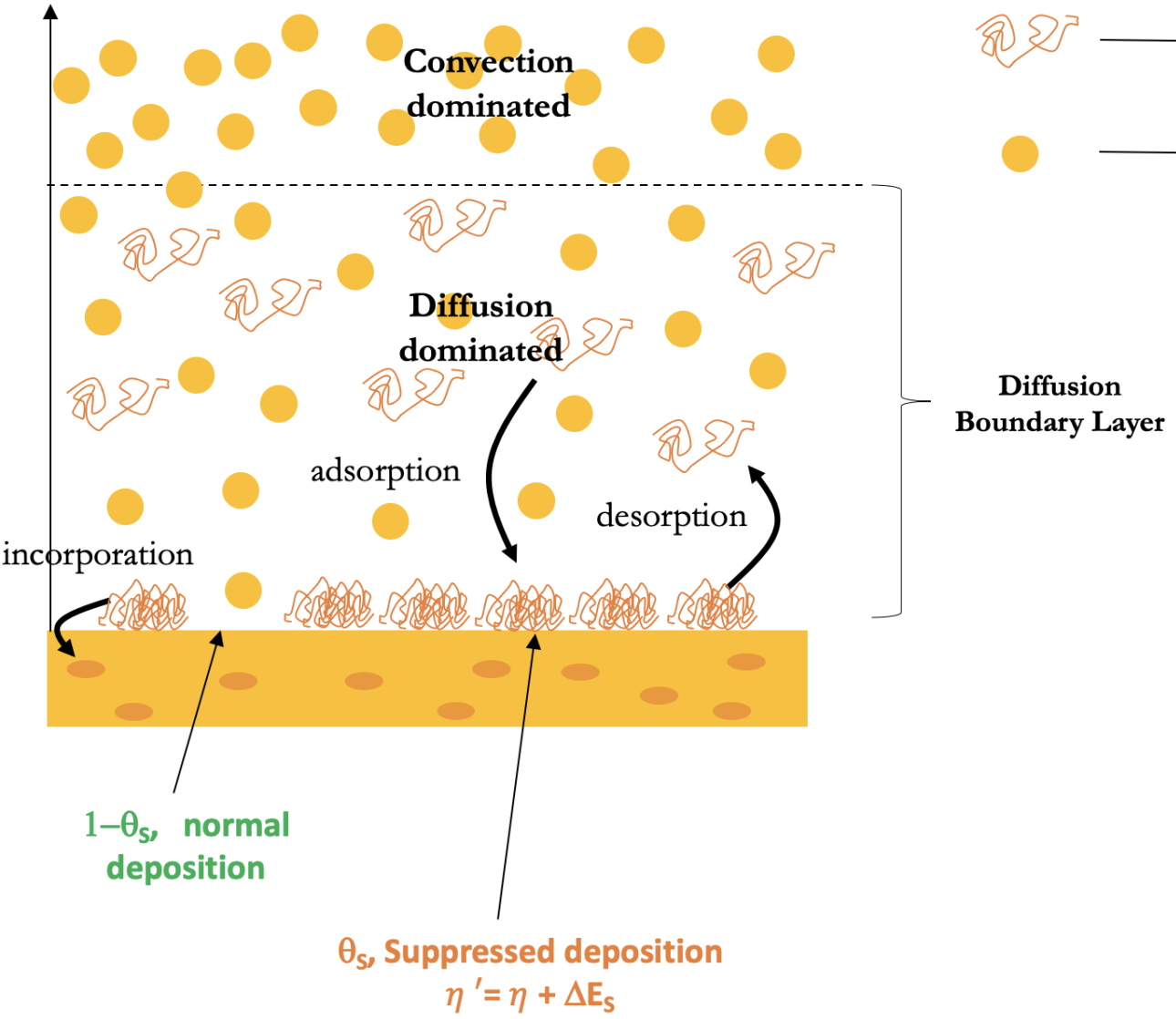

Additive molecule

Cu^{2+} ion

$$Cu^{2+} + 2\,e \rightarrow Cu$$

$$r = k_{Cu} \cdot exp(-b_{Cu} \cdot \eta) \cdot C_{Cu^{2+},x=0}$$

- Cu deposition on additive free surface fraction remains unchanged.
- Cu deposition on additive covered surface shifts by a constant over potential, ΔE_S.
- θ_S is fractional surface coverage of suppressor on surface
- Change of the coverage (t) = Adsorption – Desorption – Incorporation
- Actual scenario is far more complicated as we have three types of additives: suppressor, accelerator, leveler!

Mathematical Model

Navier-Stokes Equation:

$\boldsymbol{\rho}$, u, $\boldsymbol{\mu}$ = Density, Fluid velocity, Viscosity

$$\rho \frac{\partial u}{\partial t} + \rho(u.\nabla u) = \nabla[-pI + \mu(\nabla u + (\nabla u)^T]$$

$$\rho(\nabla . u)=0$$

Nernst-Plank Equation:

$\boldsymbol{F}$, R, T, $\boldsymbol{\varphi}$ = Faraday, Gas constant, Temperature, Electric potential field

$\boldsymbol{D_i}$, $\boldsymbol{c_i}$, $\boldsymbol{z_i}$ = Diffusion Coefficient, Concentration, valance of i^{th} ionic species

$$\frac{\partial c_i}{\partial t} = -\nabla . J$$

$$J = -D_i[\nabla c_i + u.\nabla c_i + \frac{z_i F}{RT} c_i(\nabla \varphi)]$$

Mass balance of surface coverage at cathode surface (additive cases)

Change of the coverage = Adsorption – Desorption – Consumption

$$\frac{d\theta_S}{dt} = K_{molecule\_S} \cdot \{C_S(0,t)(1-\theta_S-\theta_L)A_{AD\_S} - A_{D\_S}\theta_S - A_{\theta\_S}A_{Cu}C_{Cu}(0,t)\theta_S(1-\theta_{eq})\}$$

$$\frac{d\theta_A}{dt} = K_{molecule\_A} \cdot \{C_A(0,t)(1-\theta_A)A_{AD\_A} - A_{D\_A}\theta_A - A_{\theta\_A}A_{Cu}C_{Cu}(0,t)\theta_A(1-\theta_{eq})\}$$

$$\frac{d\theta_L}{dt} = K_{molecule\_L} \cdot \{C_L(0,t)(1-\theta_S-\theta_L)A_{AD\_L} - A_{D\_L}\theta_L - A_{\theta\_L}A_{Cu}C_{Cu}(0,t)\theta_L(1-\theta_{eq})\}$$

$$\theta_{eq} = f(\theta_S, \theta_L, \theta_A)$$

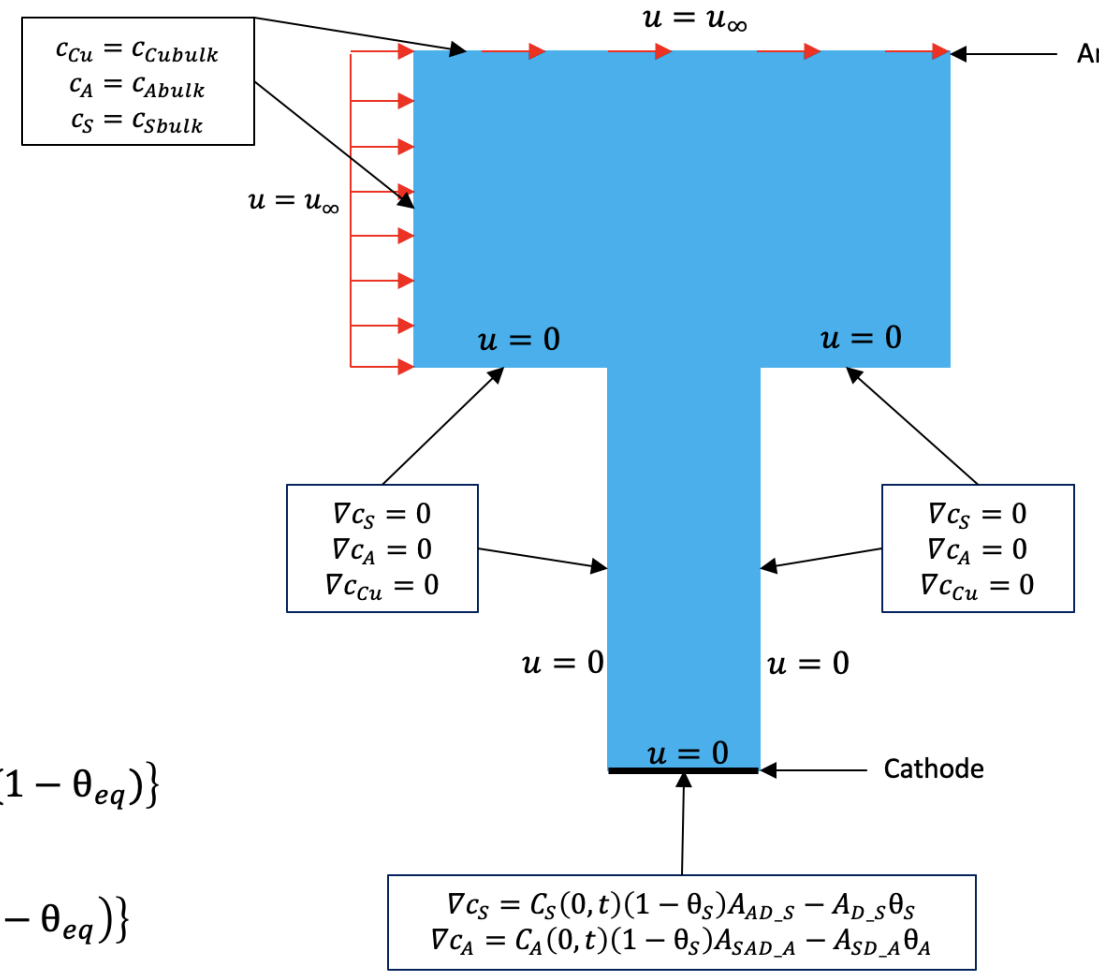

Simulation Results– Effect of Additives

- Multiphysics Problem is solved using **COMSOL Multiphysics** with Finite Element Methods
- Without additive non-uniform dome shaped deposition occurs
- Additives modify the current and hence deposition rate
- Resulting deposition profile is dependent on the chemistry of additives as well as a lot of factors including conc., viscosity etc.
- Applying a low current results in flatter deposition however needs more plating time, which is not desirable

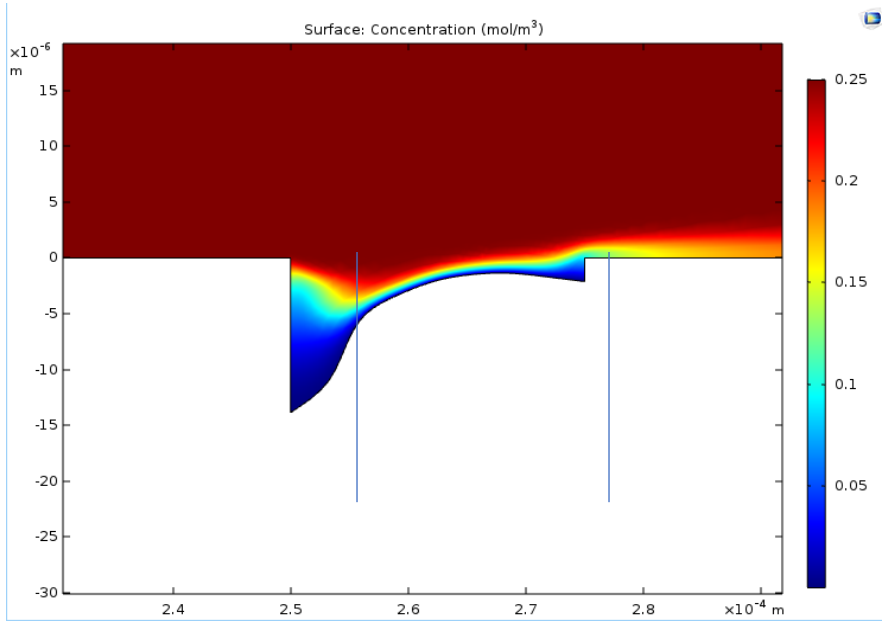

Without Additive

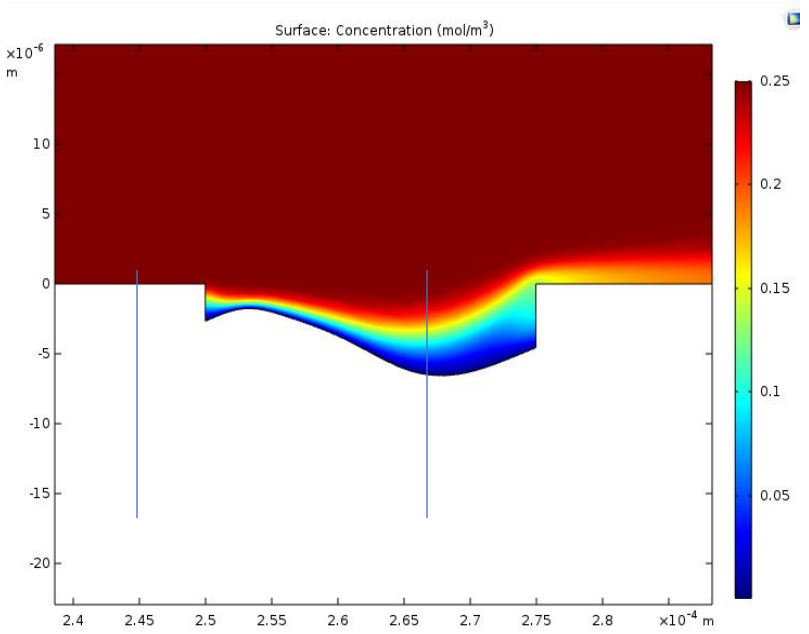

With Additives

Tribology of additively manufactured outsoles tread designs [14, 15]

Sample Preparation by Additive Manufacturing

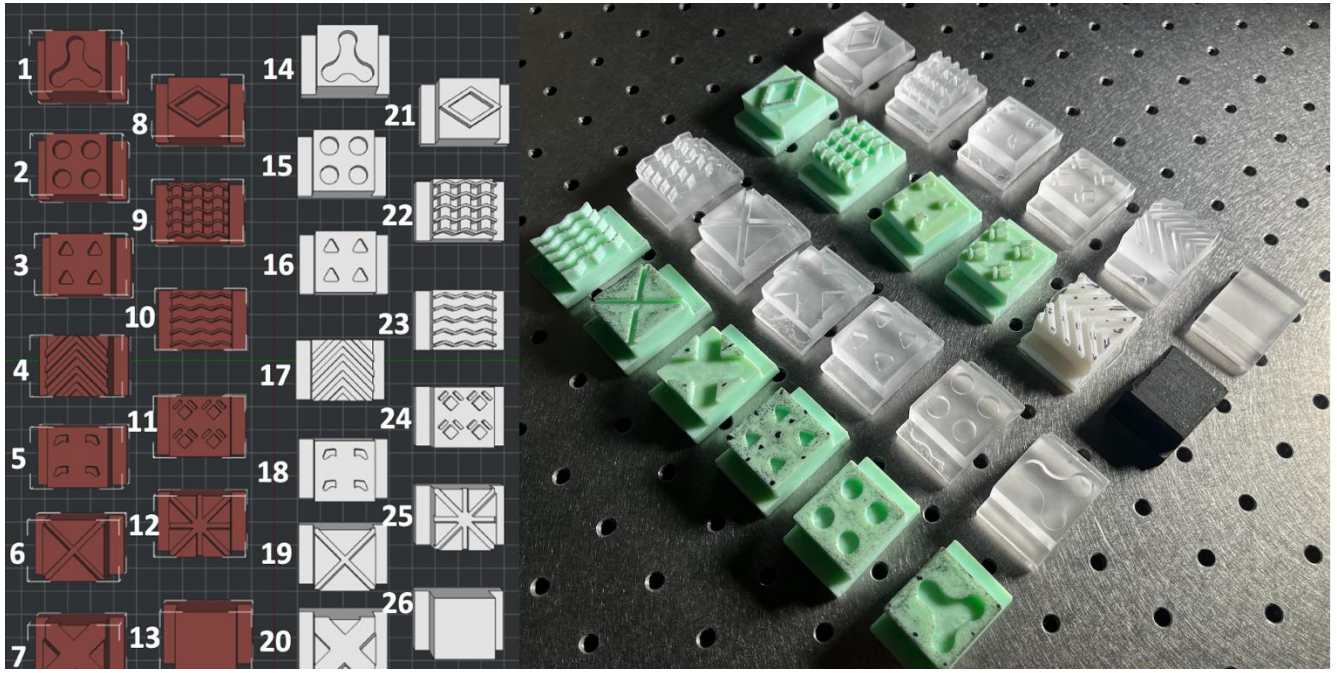

Feature	TPR (FFF)	SLA Printing
Printer Used	Atomstack Cambrian Pro	Anycubic Photon D2
Material	TPR 65A	Monocure Rapid FLEX100 Resin (50A)
Printing Process	Layer-by-layer extrusion	UV curing of liquid resin
Resolution	Moderate (0.1 mm layer thickness)	High (0.032 mm layer thickness)
Surface Finish	Textured	Smooth and high-precision
Customization	Optimized tread patterns for environments	Complex geometries, enhanced grip
Applications	Flexible and durable outsoles for varied uses	Detailed designs for sports or industrial footwear

Friction and Drainage Performance

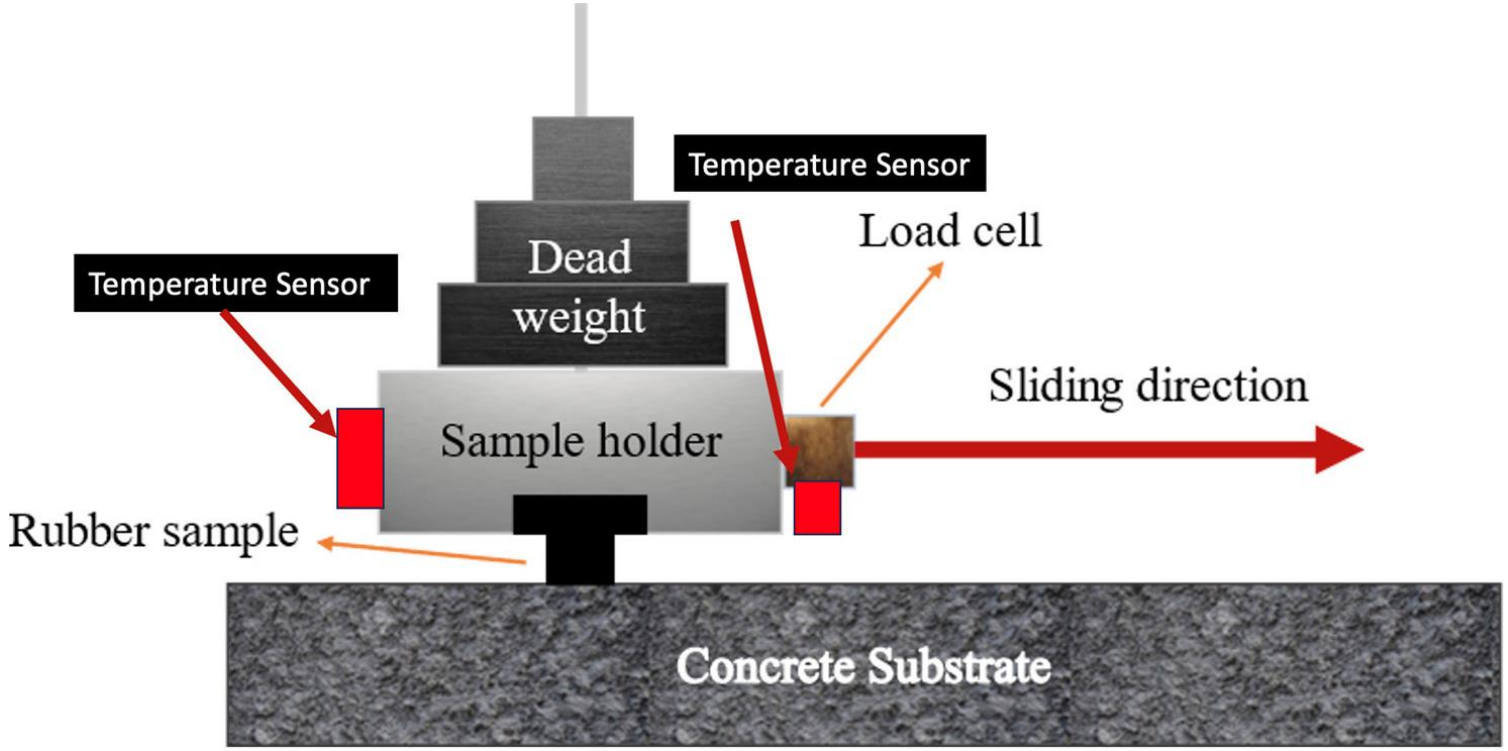

- Rubber Sample with dead weight slides on it slides
- Friction force and Temperature measured
- The loss of mass also measured in the end

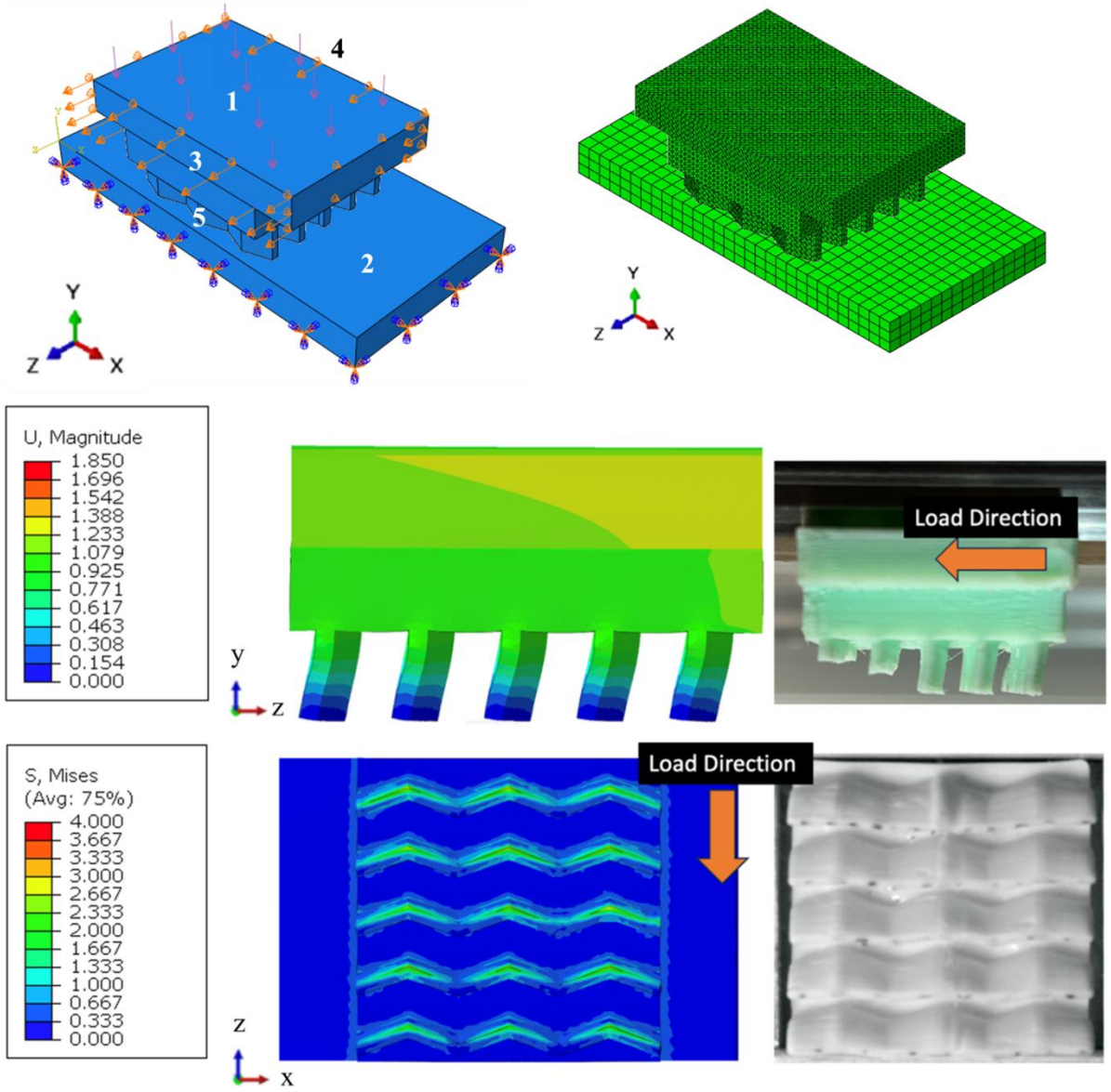

Finite Element Results compared to Experiments

SUMMARY and key Findings

- Tests: Friction/drainage on glass; wear on concrete
- Material: SLA resin → higher friction & deformation, lower wear resistance than TPR
- Tread: Larger, interconnected patterns improve traction & drainage; smooth designs underperform
- Wet: Resin retains higher friction on wet surfaces than TPR
- FEM: Ogden model captured stress hot-spots matching experiments
- Insight: Reinforce edges & optimize tread (chevron/cross) to boost durability

Gecko-Inspired Surface Microstructures: Friction Control and Adaptive Design [16]

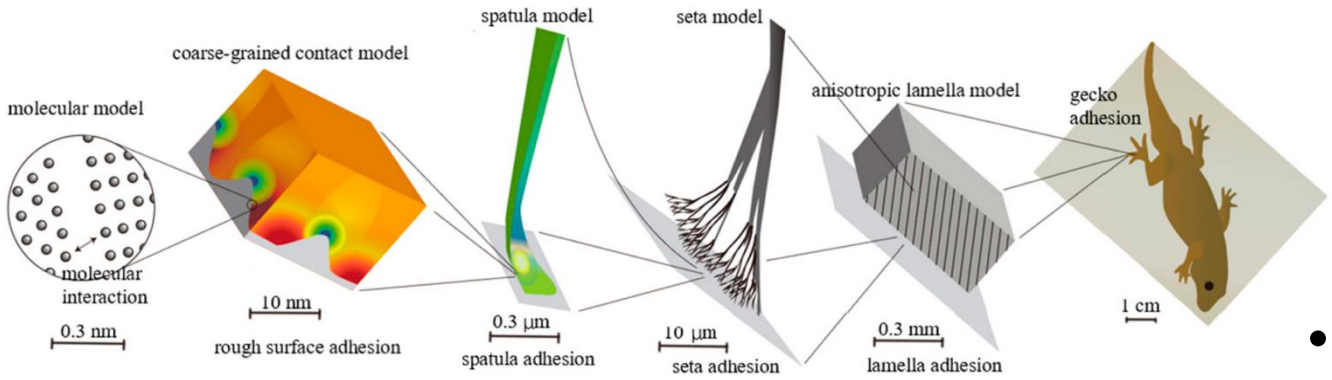

Reproduced from Roger A. Sauer [2]

RESEARCH & MOTIVATION

- **Gecko-Inspired Design Principles**
  - Microscale, hierarchical structures in gecko feet
  - Van der Waals forces → high adhesion (20 N for 200 mm²)
  - Strong, reversible attachment without adhesives
  - Works across diverse surfaces → vital for space use
- **Research Objectives**
  - 3D-print resin microstructures mimicking setae
  - Simulate behavior with FEM + hyperelastic models
  - Validate traction on rough metal surfaces
  - Optimize geometries for low-gravity conditions
- **Significance:** Breakthrough potential for robotics in space stations, satellites, and exploration vehicles

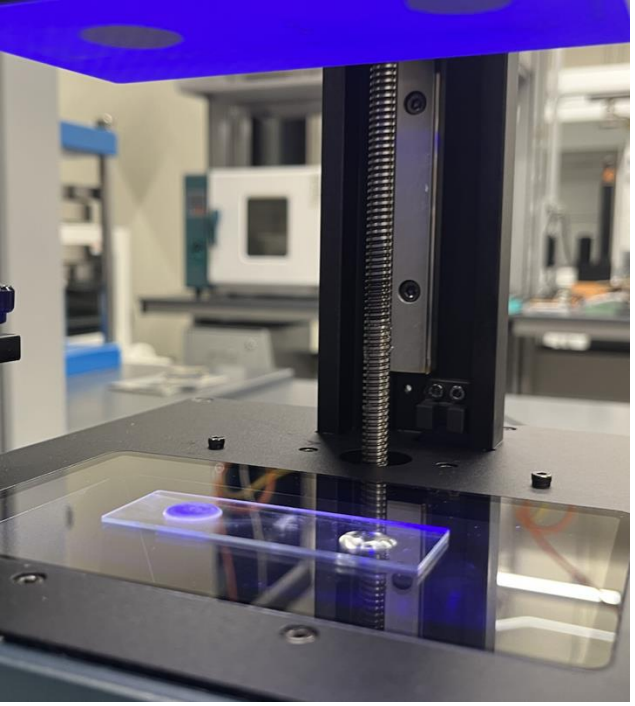

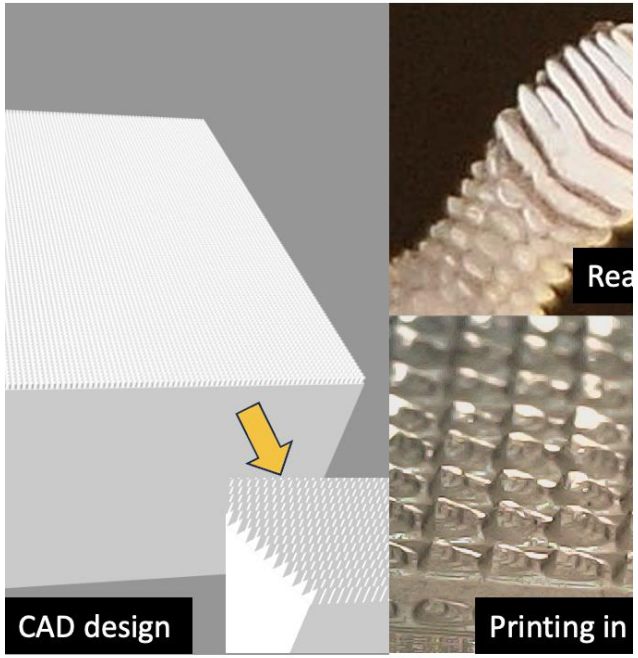

FABRICATION

SLA 3D Printing:

- Anycubic Photon D2

Material:

- FLEX100™ resin: 30-50 cps viscosity, rapid polymerization

Biomimetic Variants:

- S SPIKE: Miniaturized with highest density
- M SPIKE: Intermediate size and density
- L SPIKE: Largest with lowest density
- FLAT: Control sample

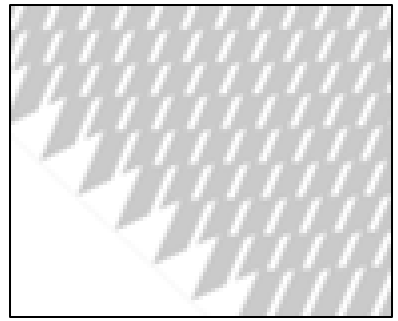

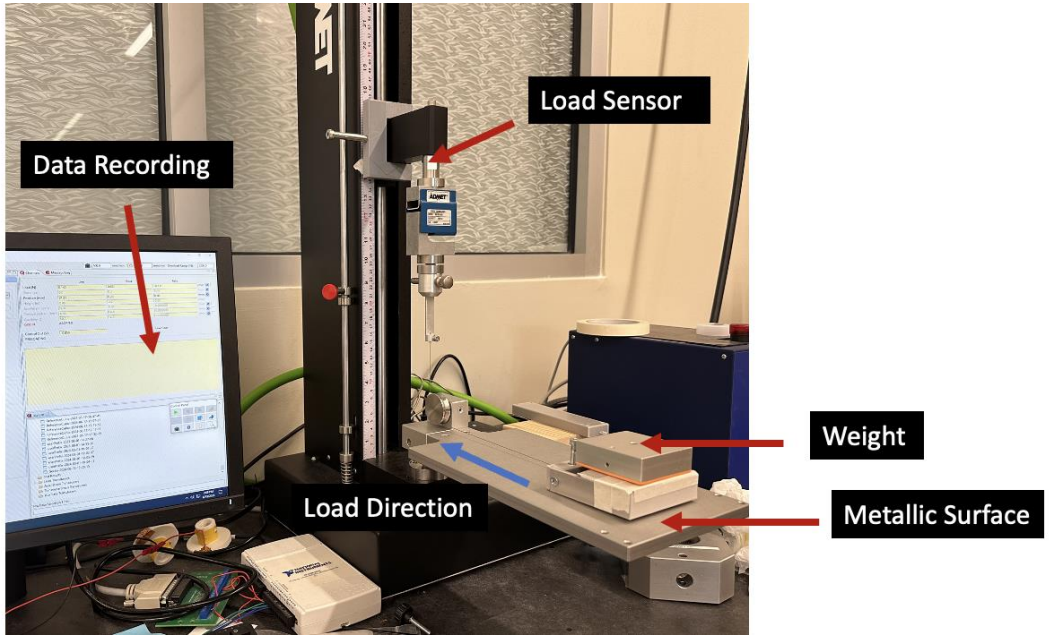

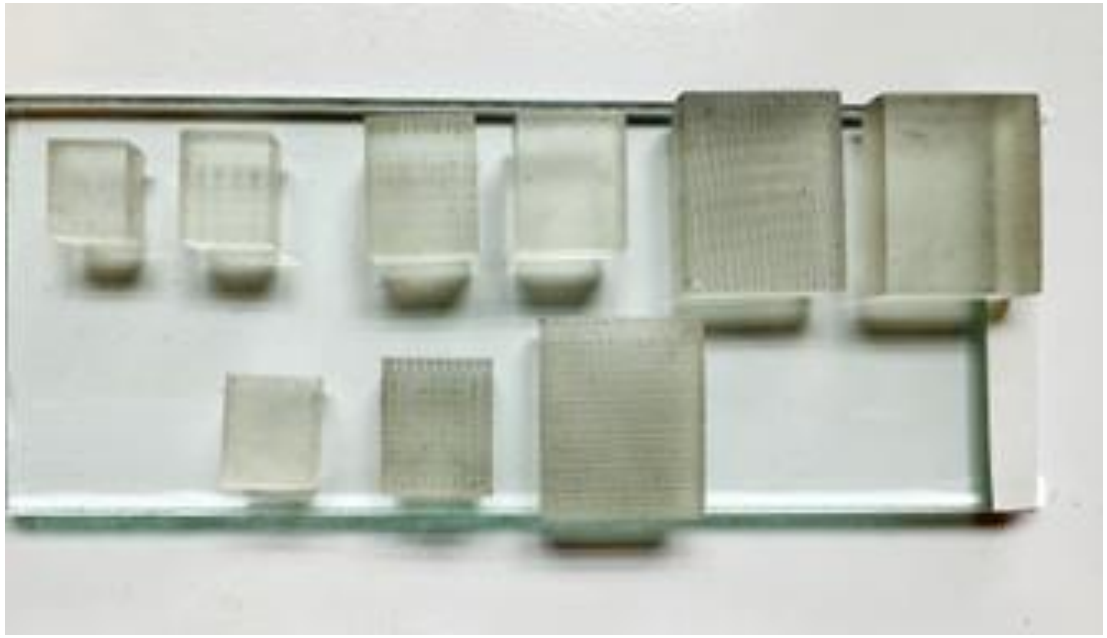

TESTING METHODOLOGY

Equipment:

- ADMET 500 Series tester with S-Type load cell (±0.25% precision)
- Custom steel wire and roller system for force measurement

Testing Protocol:

- Controlled environment: 20-25°C, 40-60% humidity
- Consistent 1.165kg normal force
- Multiple repetitions with statistical analysis

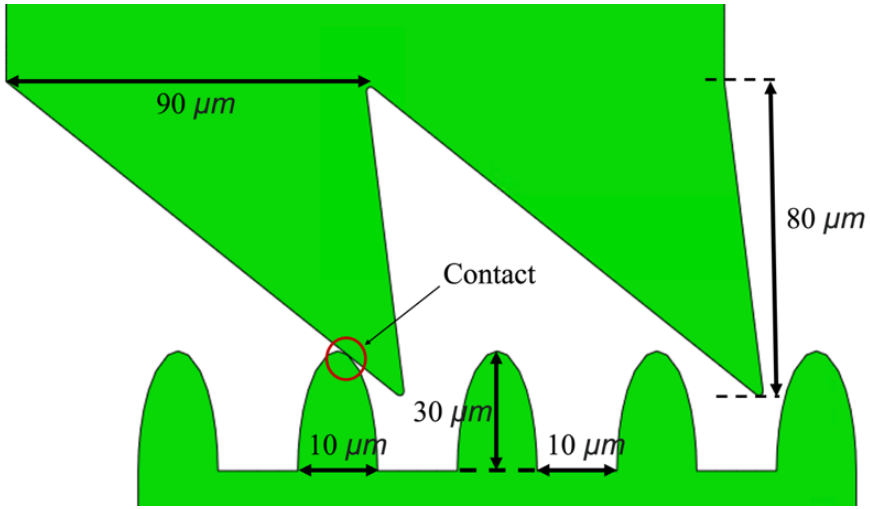

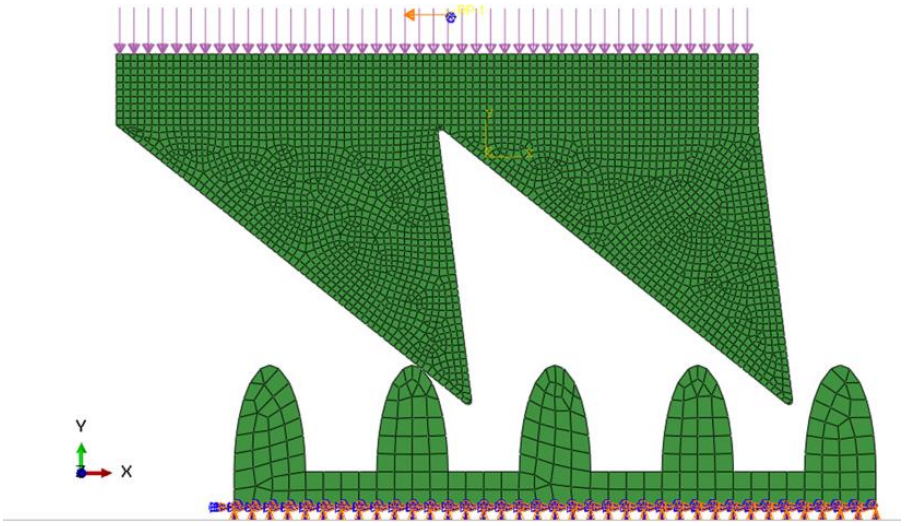

FEA SIMULATION

Model Design:

- 2D plane stress analysis with specialized elements for large deformation
- Spatulas (80μm×90μm) contacting rough surface model

Mesh Properties:

- Refined spatula mesh (3101 elements)
- Surface mesh (193 elements)

Materials:

- Surface: Elastic steel ($E=200MPa$, $\nu=0.3$)
- Spatulas: **Ogden Hyperelastic model** ($\mu_1=0.1MPa$, $\alpha_1=0.5$)

FEM SIMULATION

Multi-Step Analysis:

Contact: 10μm negative-y displacement

Compression: 0.048 micro-N pressure

Sliding: 30μm negative-x displacement

Analysis Metrics:

- Displacement fields
- Von Mises stress distribution
- Contact pressure mapping
- Shear force calculations

Quantitative Validation:

- FEM prediction for M sample: 18.6N
- Experimental measurement: 15.0N (80.6% agreement)

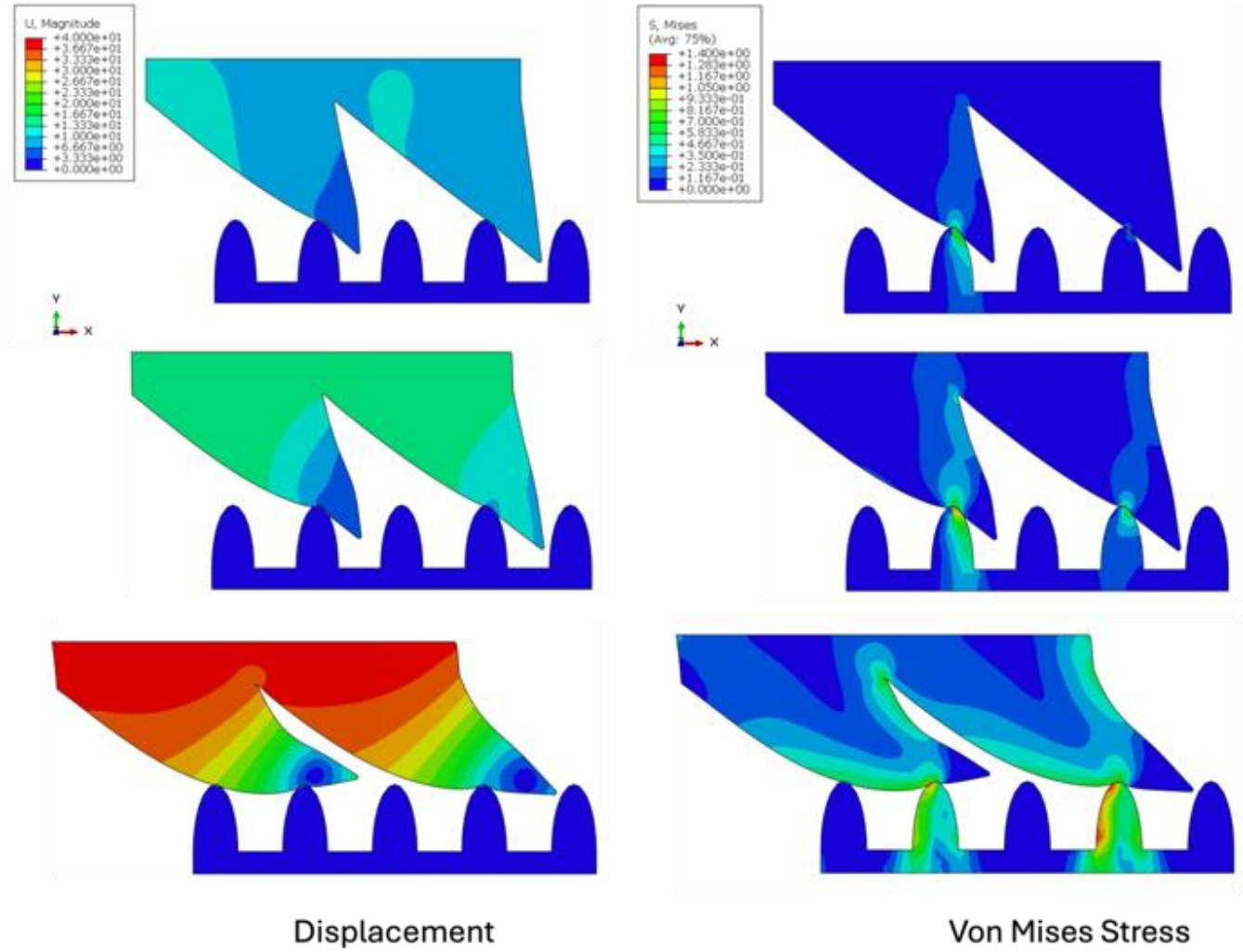

References

[1] S. De, M. Jrad, D. Locatelli, R. K. Kapania, and M. Baker, "SpaRibs geometry parameterization for wings with multiple sections using single design space," in *Proc. 58th AIAA/ASCE/AHS/ASC Structures, Structural Dynamics and Materials Conference*, Grapevine, TX, USA, Jan. 9-13 2017, Paper No. 0570.

[2] S. De, M. Jrad, D. Locatelli, R. K. Kapania, M. Baker, and C. G. Pak, "SpaRibs geometry parameterization for wings with multiple sections using single design," NASA Tech. Rep. AFRC-DAA-TN37932, Jan. 2017.

[3] S. De, M. Jrad, and R. K. Kapania, "Structural optimization of internal structure of aircraft wings with curvilinear spars and ribs," *J. Aircraft*, vol. 56, no. 2, pp. 707-718, 2019. doi: 10.2514/1.C034818

[4] M. Jrad, S. De, and R. K. Kapania, "Global-Local aeroelastic optimization of internal structure of transport aircraft wing," in *Proc. 18th AIAA/ISSMO Multidisciplinary Analysis and Optimization Conference*, Washington DC, USA, 2017, Paper No. 4321.

[5] J. H. Robinson, S. Doyle, G. Ogawa, M. Baker, S. De, M. Jrad and R. K. Kapania, "Aeroelastic optimization of wing structure using curvilinear spars and ribs (SpaRibs)," in *Proc. 17th AIAA/ISSMO Multidisciplinary Analysis and Optimization Conference*, Washington DC, USA, 2016, Paper No. 3994.

[6] S. De, K. Singh, B. Alanbay, R. K. Kapania and R. Aguero, "Structural optimization of truck front-frame under multiple load cases," in *Proc. ASME Int. Mechanical Engineering Congress & Exposition*, vol. 52187, V013T05A039, Nov. 2018.

[7] S. De, K. Singh, J. Seo, R. K. Kapania, E. Ostergaard, N. Angelini and R. Aguero, "Unconventional truck chassis design with multi-functional cross members," SAE Technical Paper 2019-01-0839, 2019.

[8] S. De, K. Singh, J. Seo, R. K. Kapania, E. Ostergaard, N. Angelini and R. Aguero, "Lightweight chassis design of hybrid trucks considering multiple road conditions and constraints," *World Electric Vehicle Journal*, vol. 12, no. 1, p. 3, 2021.

[9] S. De, W. D. Sides, T. Brusuelas and Q. Huang, "Electrodeposition of superconducting rhenium-cobalt alloys from water-in-salt electrolytes," *J. Electroanal. Chem.*, vol. 860, p. 113889, 2020.

[10] S. De, J. White, T. Brusuelas, C. Patton, A. Koh and Q. Huang, "Electrochemical behavior of protons and cupric ions in water-in-salt electrolytes with alkaline metal chloride," *Electrochimica Acta*, vol. 338, p. 135852, 2020.

[11] S. De and Q. Huang, "Mathematical modeling of cyclic voltammogram curves of copper deposition involving multiple additives," in *ECS Meeting Abstracts*, no. 28, p. 977, May 2021.

[12] Q. Huang, W. D. Sides, S. De and Y. Hu, "Electrodeposition of Cu, Co and Re from water-in-salt electrolytes," in *ECS Meeting Abstracts*, no. 46, p. 2116, Sep. 2019.

[13] S. De and Q. Huang, "Estimation of kinetic parameters of additives by semi-analytical solution," in *ECS Meeting Abstracts*, no. 17, p. 1483, Nov. 2020.

[14] S. Xu, S. De, M. Khaleghian and A. Emami, "Comparative tribological and drainage performance of additively manufactured outsoles tread designs," *Friction*, vol. 13, no. 5, 2025.

[15] S. Xu, S. De, M. Khaleghian and A. Emami, "Wear resistance of additively manufactured footwear soles," *Lubricants*, vol. 13, no. 2, p. 89, 2025.

[16] S. De, S. Xu, A. Emami and M. Khaleghian, "Gecko-Inspired surface microstructures: Friction control and adaptive design for space environments," in *ASME Aerospace Structures, Structural Dynamics, and Materials Conference*, vol. 88759, p. V001T03A023, American Society of Mechanical Engineers, 2025.

Acknowledgements

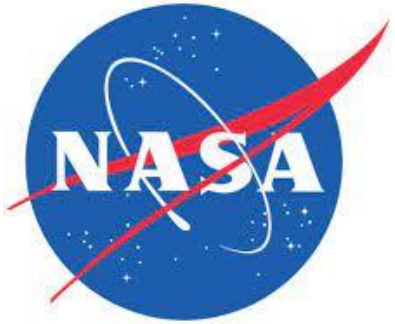

Thank you